AN ANALYSIS OF TURBULENT FLOW IN A TWO-DIMESIONAL CHANNEL

KIYOSHI MATSUMIYA, TOSHIO HAYASHI and SHIGEO UCHIDA

Department of Aeronautical Engineering

(Received October 27, 1966)

Summary

A unified velocity distribution of incompressible turbulent flow in a two-dimensional channel is calculated by making use of linear expression for shearing stress and of assumed polynomial expression for mixing length. Introducing laminar sublayer it is fairly well coincident with the law of wall and velocity defect law both in the region near wall and central region, respectively. Using these results of velocity distribution, a resistance formula is obtained, which shows fair agreement with existing measurements.

Symbols

d	half-width of the channel
l	mixing length
l_c	value of the mixing length at the center-line of the channel
p	pressure
R	Reynolds number based on mean flow velocity and channel width: $R=2u_m d/\nu$
R_s	sectional Reynolds number based on frictional velocity and channel half-width: $R_s=v_* d/\nu$
u, v	x, y components of velocity
u', v'	x, y components of velocity fluctuation
u_c	velocity at the center of channel
u_m	mean flow velocity over channel width
v_*	frictional velocity
x, y	cartesian coordinates, where x is taken parallel to the axis of channel and y normal to it measured from the wall
y_l	thickness of laminar sublayer
ζ	$=1-\eta$
η	non-dimensional distance from the wall: $\eta=y/d$
η_l	non-dimensional thickness of laminar sublayer
κ	slope of mixig length at $\eta=\eta_l$
λ	resistance coefficient : $\lambda=-\dfrac{dp}{dx}\dfrac{2d}{\frac{1}{2}\rho u m^2}$
μ	viscosity of the fluid
ν	kinemaitc viscosity
ρ	density of the fluid

σ non-dimensionalized value of mixing length at the center-line of the channel: $\sigma = l_c/d$

τ shearing stress

τ_0 shearing stress at the wall

1. Introduction

The logarithmic velocity distribution for a channel can be derived by applying Prandtl's[1] hypothesis for the turbulent shearing stress. Since it is universal in character which determined only by the wall condition and the distance from the wall, this velocity distribution is widely used as the "wall law". Though the idea of laminar sublayer is introduced, this "wall law" does not satisfy the boundary conditions at the center-line of the channel and, therefore, it can not be applied to the whole section.

In the center-line region of a channel a similarity rule called "velocity-defect law" was established by von Kârmân[2]. This is also universal in character but can not apply to the wall region.

These formulae have been verified by many experiments, for example, by Nikuradse[3], Laufer[4] for a channel flow and by the same authors[5,6] for a circular pipe flow. As it is shown by experiments each curve of these formulae can not cover the whole section of a turbulent channel. Full profile for channel or pipe flow has been presented by Reichardt[7] and Deissler[8] by introducing the turbulent viscosity coefficient and Szablewski[9] has also presented a full profile for pipe flow by combining these formulae. Pai[10] has tried another attempt by solving the Reynolds equation and obtained a full profile.

In order to obtain a resistance formula for a channel, it is necessary to know the velocity distribution through whole section of a channel. Under the assumption that the laminar friction was negligible compared with the turbulent one, Prandtl[11] has derived the universal resistance law for pipe flow from the logarithmic velocity distribution.

Considering these situations it will be necessary to derive the unified theory to describe the full profile of a turbulent channel flow. In this connection present authors intended to develope a new expression of full profile, which enables us to calculate the resistance formula. The basic concept of previous work[12] on turbulent boundary layer along a flat plate has been reffered to the present one. Applying the linear distribution for shearing stress and assumed polynomial expression for mixing length to Prandtl's[1] hypothesis, full profile of velocity distribution has been derived, which satisfies the boundary conditions at both ends. The resistance formula is easily calculated by the use of the relation between the shearing stress and Reynolds number derived from velocity distributions.

The major part of calculation can not be expressed in closed form and numerical process has often been employed. The result shows fair agreement with the existing measurements[3,4,13,14].

2. Shearing Stress

The two dimensional flow of incompressible fluid in a channel is concerned. Taking coordinate x parallel to the axis of a channel and y normal to it, the

fluid is governed by continuity equation and equations of motion with the boundary layer approximation :

$$\frac{\partial u}{\partial x}+\frac{\partial v}{\partial y}=0 \tag{1}$$

$$\rho u\frac{\partial u}{\partial x}+\rho v\frac{\partial u}{\partial y}=-\frac{\partial p}{\partial x}+\frac{\partial \tau}{\partial y} \tag{2}$$

$$\frac{\partial p}{\partial y}=0 \tag{3}$$

where u, v are x, y components of the velocity, respectively. Density ρ is constat and pressure p is an only function of x.

Assuming that the flow has velocity component along x-axis only, the variations of velocity with x have vanished from Eq. (1). This corresponds to the condition of fully developed turbulent flow. In this situation, it is given from Eq. (2):

$$\frac{\partial \tau}{\partial y}=\frac{dp}{dx} \tag{4}$$

Integration of Eq. (4) with y gives:

$$\tau=-\frac{dp}{dx}(d-y) \tag{5}$$

where d denotes the half-width of a channel. Nondimensionalizing Eq. (5) with the wall shearing stress τ_0, we have

$$\frac{\tau}{\tau_0}=1-\eta \tag{6}$$

where $\eta=y/d$.

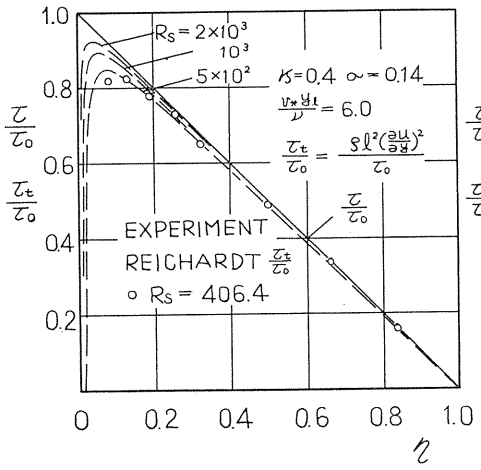

FIG. 1. Distribution of shearing stress for $v_* y_1/\nu=6$.

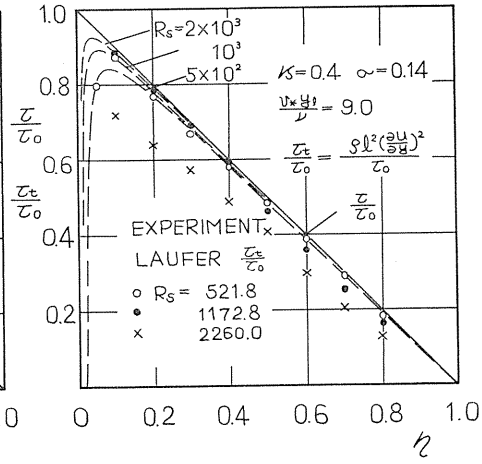

FIG. 2. Distribution of shearing stress for $v_* y_1/\nu=9$.

This linear distribution of shearing stress is given in Fig. 1 and 2 where other curves show the component of turbulent shear stress which is calculated in the following sections. Comparing the caluculated turbulent stress with the experimental data by Reichardt[13] and Laufer[4], the present profile seems to be a reasonable one.

3. Mixing Length

The laminar sublayer of thickness y_l is considered, where y_l is assumed to change by the following law :

$$v_* y_l/\nu \equiv A = \text{const} \tag{7}$$

where $v_* = \sqrt{\tau_0/\rho}$ denotes the frictional velocity and ν the kinematic viscosity. In the following calculation, $A=6$ and 9 are assumed for two different channel flows. Assuming that the mixing length is vanished in laminar sublayer and refering to the experimental results[3][5], which show that the mixing length tends to a finite value close to the center-line of a channel, the following boundary conditions are imposed:

$$\left.\begin{array}{lll} l=0, & dl/dy=\kappa & \text{at } y=y_l \\ il=i_c l_c, & dl/dy=0 & \text{at } y=d \end{array}\right\} \tag{8}$$

We assume now an expression in series expansion up to the third degree for the mixing length in order to satisfy the boundary conditions. Applying Eq. (8)

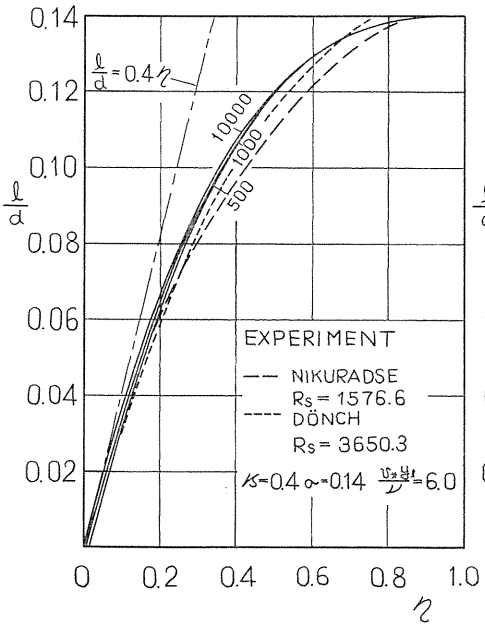

FIG. 3. Distribution of mixing length for $v_* y_l/\nu=6$.

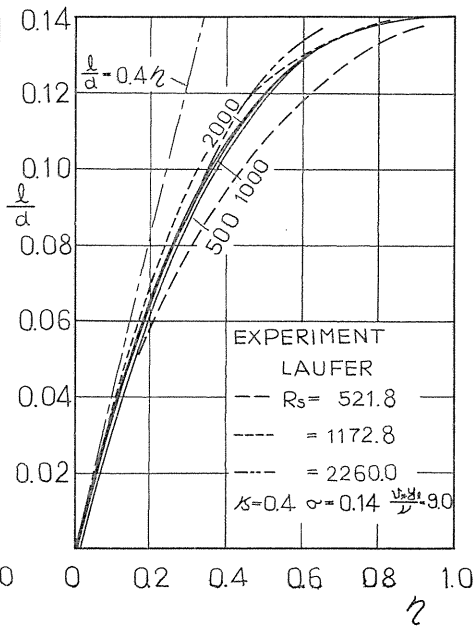

FIG. 4. Distribution of mixing length for $\nu_* y_l/\nu=9$.

to this expression, coefficients are determined as follows:

$$l/d = \sigma + C_2(1-\eta)^2 + C_3(1-\eta)^3$$
$$= (\sigma + C_2 + C_3) - (2C_2 + 3C_3)\eta + (C_2 + 3C_3)\eta^2 - C_3\eta^3 \tag{9}$$

where $\sigma = l_c/d$, $\eta_l \equiv y_l/d = A \Big/ \left(\frac{v_* d}{\nu}\right)$ and

$$C_2 = \frac{\kappa(1-\eta_l) - 3\sigma}{(1-\eta_l)^2}, \quad C_3 = -\frac{\kappa(1-\eta_l) - 2\sigma}{(1-\eta_l)^3}$$

A sectional Reynolds number is introduced here, defining

$$R_s = \frac{v_* d}{\nu} \tag{10}$$

It will be seen that the mixing length is a function of parameter κ, σ, A and R_s. In the present calculation, $\kappa=0.4$, $\sigma=0.14$, $A=6$ and 9 are employed.

Comparing with the measurements by Nikuradse[3], Dönch[14] and Laufer[4], the present expression seems to be valid as shown in Fig. 3 and 4.

4. Velocity Distributions

The equation of motion for the mean velocity in a turbulent flow is derived from Navier-Stokes equation. Applying the boundary layer approrimation, it is given:

$$\rho u \frac{\partial u}{\partial x} + \rho v \frac{\partial u}{\partial y} = -\frac{\partial p}{\partial x} + \frac{\partial}{\partial y}\left[\mu \frac{\partial u}{\partial y} - \rho \overline{u'v'}\right] \tag{11}$$

where u' and v' are the velocity fluctuations in x and y directions, respectively. Comparing this Reynolds equation with Eq. (1), we can find that the general expression for shearing stress is considered as the sum of molecular shear and Reynolds stress as follows:

$$\tau = \mu \frac{\partial u}{\partial y} - \rho \overline{u'v'} \tag{12}$$

Within a laminar sublayer, the turbulent fluctuations are assumed to be decayed off and, therefore, it is given from Eq. (12):

$$\tau = \mu \frac{\partial u}{\partial y} \tag{13}$$

Non-dimensionalized velocity gradient is obtained by Eq. (13). Putting Eq. (6) we have

$$\frac{\partial(u/v_*)}{\partial(y/d)} = \frac{v_* d}{\nu} \frac{\tau}{\tau_0} = R_s(1-\eta) \tag{14}$$

Integration of Eq. (14) with the boundary condition, $u=0$ at $\eta=0$, gives the velocity distribution in laminar sublayer:

$$\frac{u}{v_*} = R_s\left(\eta - \frac{1}{2}\eta^2\right) \tag{15}$$

In the major part of the flow outside a laminar sublayer, Eq. (12) must be used for the expression of the shearing stress. Applying the momentum transfer theory to Reynolds stress term, it is given:

$$\tau = \mu\frac{\partial u}{\partial y} + \rho l^2\left(\frac{\partial u}{\partial y}\right)^2 \tag{16}$$

Eq. (16) is solved to give the following result:

$$\frac{\partial u}{\partial y} = \sqrt{\frac{\tau}{\rho l^2} + \frac{\nu^2}{4\,l^4}} - \frac{\nu}{2\,l^2}$$

Putting it in the non dimensional form:

$$\frac{\partial(u/v_*)}{\partial(y/d)} = \sqrt{\frac{\tau/\tau_0}{(l/d)^2} + \frac{1}{4\,R_s^2(l/)^4 d}} - \frac{1}{2R_s(l/d)^2} \tag{17}$$

Substituting Eqs. (6) and (9) with fixed value of $\kappa=0.4$ and $\sigma=0.14$ Eq. (17) can be integrated numerically to give the velocity distribution at $\eta \geqq \eta_l$. The initial value u_l at $\eta=\eta_l$ is introduced from Eq. (15):

$$\frac{u_l}{v_*} = R_s\left(\eta_l - \frac{1}{2}\eta_l^2\right) \tag{18}$$

At the edge of laminar sublayer the mixing length tends to be zero, while the shearing stress is finite, and therefore the velocity gradient in Eq. (17) has an expression $\infty - \infty$. But it is easily shown that the gradient tends to the finite value by the use of series expansion.

$$\frac{\partial(u/v_*)}{\partial(y/d)} = R_s\frac{\tau}{\tau_0} - R_s\left(R_s\frac{\tau}{\tau_0}\right)^2\left(\frac{l}{d}\right)^2 + 2\,R_s^2\left(R_s\frac{\tau}{\tau_0}\right)^3\left(\frac{l}{d}\right)^4 + \cdots \tag{19}$$

It can be integrated in the region very close to laminar sublayer:

$$\frac{u}{v_*} = \frac{u_l}{v_*} + a_1(\eta - \eta_l) + a_2(\eta - \eta_l)^2 + a_3(\eta - \eta_l)^3 + a_4(\eta - \eta)^4 + \cdots \tag{20}$$

where

$$a_1 = R_s(1 - \eta_l), \quad a_2 = -\frac{R_s}{2}, \quad a_2 = -\frac{R_s^3\kappa^2}{3}(1 - \eta_l)^2$$

$$a_4 = -\frac{R_s^3\kappa}{2}(1 - \eta_l)\{k(1 - \eta_l) - \kappa\}, \quad k \equiv -\frac{2\,\kappa\,(1 - \eta_l) - 3\,\sigma}{(1 - \eta_l)^2}$$

It is seen from Eq. (20) that the velocity distribution at the outer edge of laminar sublayer also tends to a finite value u_l/v_*.

The integration through full section:

$$\int_0^1 \frac{\partial(u/v_*)}{\partial(y/d)}\,d\eta = \frac{u_c}{v_*} \tag{21}$$

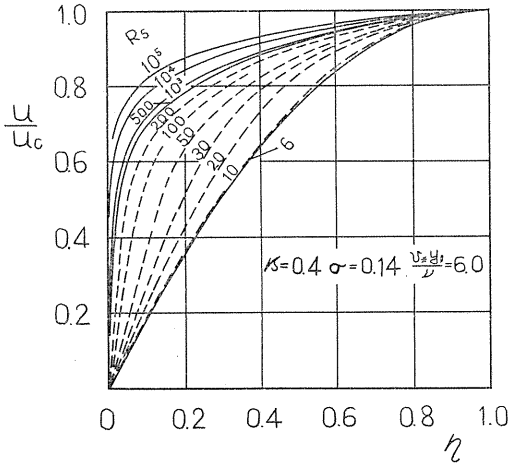

FIG. 5. Velocity distribution.

TABLE-1. Velocity Profile ($v_* y_l/\nu = 6$)

$R_s = 500$			$R_s = 10^3$		
y/d	u/v_*	u/u_c	y/d	u/v_*	u/u_c
			0	0	0
			0.006	5.982	0.2675
			0.008	7.705	0.3446
0.012	5.964	0.2911	0.01	8.82$\bar{5}$	0.3947
0.016	7.677	0.3747	0.015	10.46	0.4680
0.02	8.791	0.4291	0.02	11.45	0.5121
0.03	10.43	0.5089	0.04	13.56	0.606$\bar{5}$
0.04	11.41	0.5571	0.06	14.70	0.6574
0.06	12.68	0.6189	0.08	15.49	0.6928
0.08	13.53	0.6602	0.1	16.10	0.7199
0.14	15.11	0.7377	0.15	17.20	0.7693
0.2	16.11	0.7865	0.2	17.99	0.8046
0.4	18.09	0.8831	0.4	19.96	0.892$\bar{5}$
0.6	19.28	0.9411	0.6	21.15	0.9457
0.8	20.09	0.9804	0.8	21.96	0.9819
1.0	20.49	1.0	1.0	22.36	1.0

$R_s = 2 \times 10^3$			$R_s = 5 \times 10^3$		
y/d	u/v_*	u/u_c	y/d	u/v_*	u/u_c
0	0	0	0	0	0
			0.0012	5.996	0.2248
0 003	5.991	0.2479	0.0016	7.728	0.2897
0.005	8.842	0.3658	0 002	8.852	0.3319
0.0135	12.42	0.5139	0.003	10.49	0.393$\bar{5}$
0.02	13.58	0.5617	0.004	11.48	0.4305
0.04	15.49	0.6410	0.013	15.06	0.5647
0.06	16.58	0.6859	0.022	16.47	0.6174
0.08	17.34	0.7175	0.031	17.37	0.6511
0.1	17.94	0.7421	0.04	18.03	0.6760
0.15	19.02	0.7871	0.12	20.94	0.7850
0.2	19.81	0.8194	0.2	22.31	0.836$\bar{5}$
0.4	21.76	0.9004	0.4	24.26	0.9096
0.6	22·95	0.9496	0.6	25.45	0.9542
0.8	23.76	0.9831	0.8	26.26	0.9847
1.0	24.17	1.0	1.0	26.67	1.0

TABLE-1. *Continued*

$R_s=10^4$			$R_s=2\times10^4$		
y/d	u/v_*	u/u_c	y/d	u/v_*	u/u_c
0	0	0	0	0	0
			0.0003	5.999	0.1999
0.0006	5.998	0.2115	0.0005	8.819	0.2938
0.0008	7.731	0.2726	0.0007	10.21	0.3401
0.001	8.855	0.3123	0.002	13.55	0.4515
0.002	11.51	0.4057	0.004	15.45	0.5148
0.003	12.76	0.4501	0.006	16.52	0.5504
0.005	14.22	0.5016	0.008	17.27	0.5753
0.007	15.14	0.5339	0.01	17.84	0.594$\bar{5}$
0.0235	18.37	0.6478	0.02	19.62	0.6536
0.04	19.74	0.6961	0.04	21.39	0.7127
0.12	22.63	0.7979	0.1	23.76	0.7915
0.2	24.00	0.8462	0.2	25.60	0.8530
0.4	25.9$\bar{5}$	0.9150	0.4	27.58	0.9188
0.6	27.14	0.9569	0.6	28.79	0.9593
0.8	27.9$\bar{5}$	0.9856	0.8	29.60	0.9864
1.0	28.36	1.0	1.0	30.01	1.0

$R_s=5\times10^4$			$R_s=10^5$		
y/d	u/v_*	u/u_c	y/d	u/v_*	u/u_c
0	0	0	0	0	0
0 00012	6.000	0.1851	0.00006	6.000	0.175$\bar{5}$
0 00016	7.733	0.2386	0.00008	7.79$\bar{5}$	0.2279
0.0002	8.858	0.2733	0.0001	8.920	0.2608
0.0003	10.50	0.3240	0.0002	11.57	0.3383
0.0004	11.49	0.354$\bar{5}$	0.0003	12.83	0.3751
0 0013	15.01	0.4632	0.0005	14.29	0.4178
0.0022	16.41	0.5063	0.0007	15.20	0.4446
0.0031	17.30	0.5337	0.00235	18.42	0.5386
0.004	17.95	0.5540	0.004	19.77	0.5782
0.012	20.78	0.6413	0.012	22.58	0.6603
0.02	22.08	0.6812	0.02	23.87	0.6980
0.04	23.84	0.7357	0.04	25.63	0.7495
0.06	24.88	0.7677	0 06	26.67	0.7799
0.08	25.62	0.7906	0 08	27.41	0.8016
0.1	26.20	0 8085	0.1	27.99	0.8185
0.15	27.27	0.8416	0.15	29.06	0.8498
0.2	28.0$\bar{5}$	0.865$\bar{5}$	0.2	29.84	0.872$\bar{5}$
0.4	30.00	0.9256	0.4	31.78	0.929$\bar{5}$
0.6	31.19	0.9623	0.6	32.97	0.9643
0.8	32.00	0.9874	0.8	33.79	0.9880
1.0	32.41	1.0	1.0	34.20	1.0

gives an important factor u_c/v_*, which is directly connected with the resistance coefficient as shown in the next paragraph. Dividing the velocity distribution u/v_* by u_c/v_*, we have the full profile of velocity u/u_c as the function of y/d. The results are shown in Fig. 5 and are tabulated in Table 1 and 2.

Comparing the present velocity profile with experiments[3)4)13)14)], it shows fairly good agreement as shown in Fig. 6 and 7. The logarithmic representation of velocity profile is shown in Fig. 8. We can see from Fig. 8 that the velocity

TABLE-2. Velocity Profile ($v^*y_l/\nu=9$)

$R_s=500$			$R_s=10^3$		
y/d	u/v_*	u/u_c	y/d	u/v_*	u/u_c
0	0	0	0	0	0
			0.009	8.960	0.3540
			0.011	10.68	0.4219
0.018	8.919	0.3815	0.013	11.80	0.4661
0.022	10.62	0.4544	0.023	14.44	0.570$\bar{5}$
0.026	11.73	0.5018	0.033	15.70	0.6203
0.046	14.36	0.6144	0.053	17.17	0.6784
0.066	15.63	0.6684	0.073	18.10	0.7151
0.086	16.47	0.7044	0.093	18.78	0.7422
0.106	17.10	0.7316	0.113	19·33	0.7638
0.153	18.19	0·7779	0.1565	20.23	0.7996
0.2	18.96	0.8110	0.2	20.92	0.8266
0.4	20.97	0.8972	0.4	22.90	0.9048
0.6	22.17	0.9484	0.6	24.09	0.9520
0.8	22.98	0.9828	0.8	24.90	0.9840
1.0	23.38	1.0	1.0	25.31	1.0

$R_s=2\times10^3$			$R_s=5\times10^3$		
y/d	u/v_*	u/u_c	y/d	u/v_*	u/u_c
0	0	0	0	0	0
0.0045	8.980	0.3310	0.0018	8.992	0.3036
0.0055	10.71	0.3946	0.0022	10.84	0.3659
0.0065	11.83	0.4360	0.0026	11.96	0.4038
0.0075	12.61	0.4649	0.0046	14.61	0.4932
0.0085	13.21	0.4870	0.0066	15.87	0.5358
0.0095	13.70	0.5049	0.0086	16.70	0.5639
0.0105	14.10	0.5198	0.0106	17.33	0.5850
0.01525	15.45	0.5696	0.0153	18.38	0.620$\bar{5}$
0.02	16.32	0.6018	0.02	19.12	0.6454
0.04	18.36	0.6769	0.04	20.98	0.7082
0.06	19.48	0.7182	0.06	22.04	0.7443
0.08	20.26	0.7470	0.08	22.80	0.7699
0.1	20.87	0.7692	0.1	23.39	0.7898
0.15	21.97	0.8097	0.15	24.47	0.8263
0.2	22.75	0.8388	0.2	25 25	0.8526
0.4	24.72	0.9112	0.4	27.21	0.9186
0.6	25.91	0.9551	0.6	28.40	0.9588
0.8	26.72	0.9850	0.8	29.21	0.9862
1.0	27.13	1.0	1.0	29.62	1.0

$R_s=10^4$			$R_s=10^4$		
y/d	u/v_*	u/u_c	y/d	u/v_*	u/u_c
0	0	0	0.02	20.85	0.6671
0.0009	8.996	0.2878	0.04	22.66	0.7250
0.0011	10.73	0.3432	0.06	23.71	0.7586
0.0013	11.85	0.3792	0.08	24.46	0.7826
0.0023	14.50	0.4640	0.1	25.04	0.8013
0.0033	15.76	0.5043	0.15	26.12	0.8356
0.0053	17.22	0.5510	0.2	26.89	0.8604
0.0073	18.14	0.5803	0.4	28.84	0.9228
0.0093	18.81	0.6017	0.6	30.03	0.9609
0.0113	19.34	0.6187	0.8	30.84	0.9869
0.01565	20.20	0.646$\bar{5}$	1.0	31.25	1.0

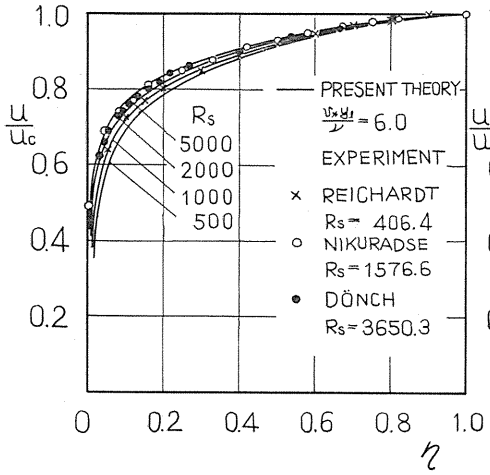

FIG. 6. Velocity distribution compared with experiments for $v_* y_l/\nu = 6$.

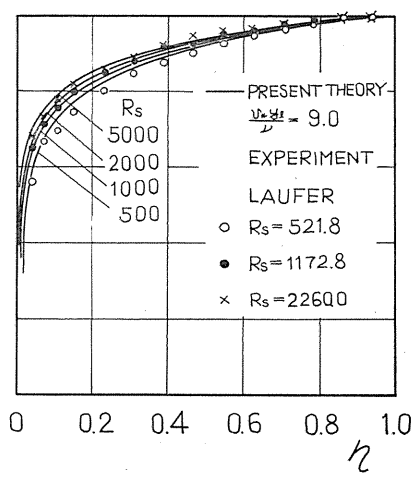

FIG. 7. Velocity distribution compared with experiments for $v_* y_l/\nu = 9$.

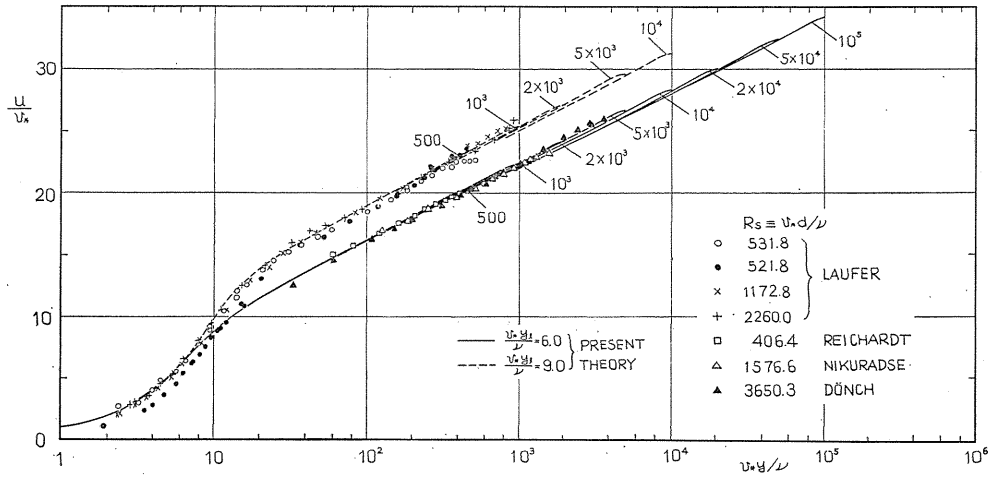

FIG. 8. Logarithmic representation of velocity distributions.

distribution has a close relation with logarithmic law in the intermediate region of $v_* y/\nu$.

In order to examine the velocity distribution on the basis of the velocity defect law, $(u_c - u)/v_*$ is calculated and shown in Fig. 9 and 10. Its logarithmic representation is given in Fig. 11 and 12. It is found that in $R_s \geqq 10^3$ the present theory produces neary single relation between $(u_c - u)/v_*$ and y/d in the central region. This fact seems to illustrate the validity of velocity defect law in the present calculation.

The velocity distribution near the center-line region can be examined in the following. Putting

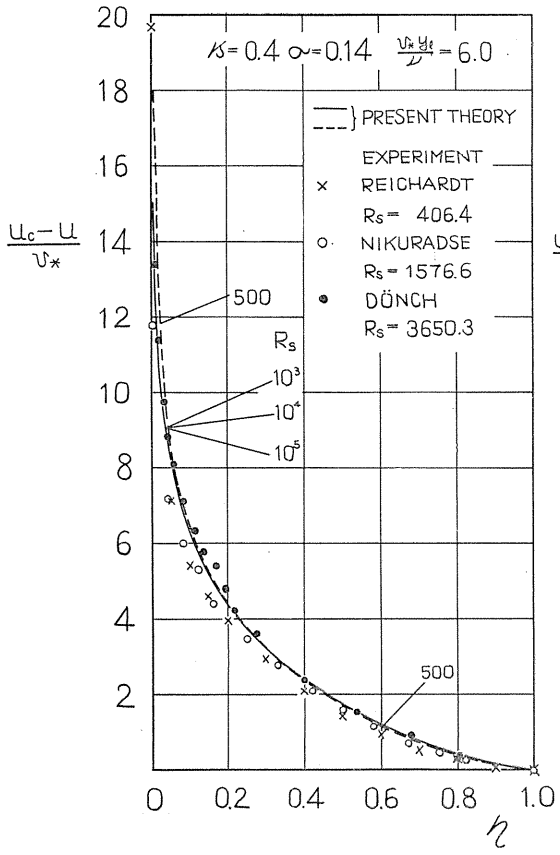

FIG. 9. Expression of velocity defect law for $v^*y_l/\nu=6$.

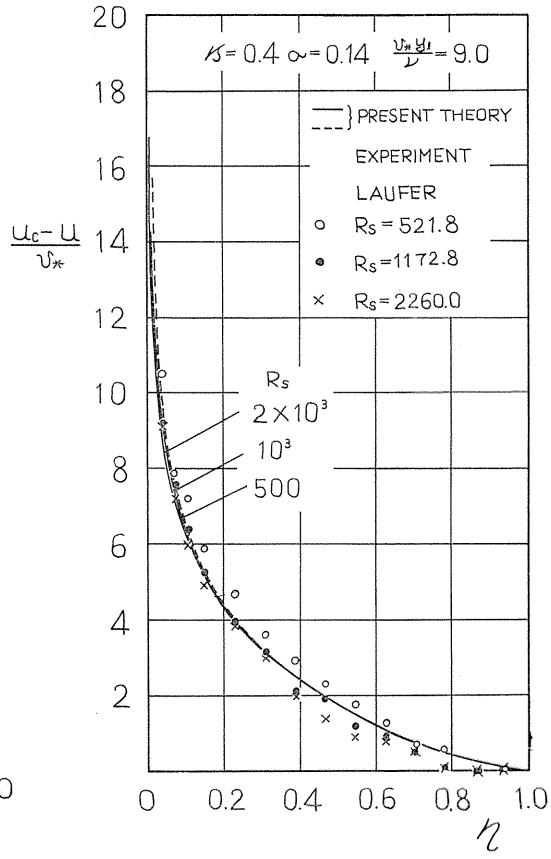

FIG. 10. Expression of velocity defect law for $v_*y_l/\nu=9$.

$$\zeta = 1 - \eta$$

into Eqs. (6) and (9) we have

$$\tau/\tau_0 = \zeta \tag{22}$$

$$l/d = \sigma + C_2\zeta^2 + C_3\zeta^3 \tag{23}$$

Eq. (17) can be deformed by Taylor expansion respecting ζ as follows:

$$-\frac{\partial(u/v_*)}{\partial\zeta} = R_s\zeta - R_s^3\sigma^2\zeta^2 + 2\,R_s^5\sigma^4\zeta^3 + \cdots \tag{24}$$

Integration of Eq. (24) with the boundary condition, $u=u_c$ at $\zeta=0$, gives

$$\frac{u_c - u}{v_*} = \frac{R_s}{2}\zeta^2 - \frac{R_s^3\sigma^2}{3}\zeta^3 + \frac{R_s^5\sigma^4}{2}\zeta^4 + \cdots \tag{25}$$

Comparing this result with that of boundary layer along a flat plate, it is seen that $(u_c-u)v_*$ is varied as ζ^2 in a channel flow, while it changes as ζ^3 in a boundary layer flow. This difference seems to be mostly due to a sensitivity to conditions at the outer edge $y=d$.

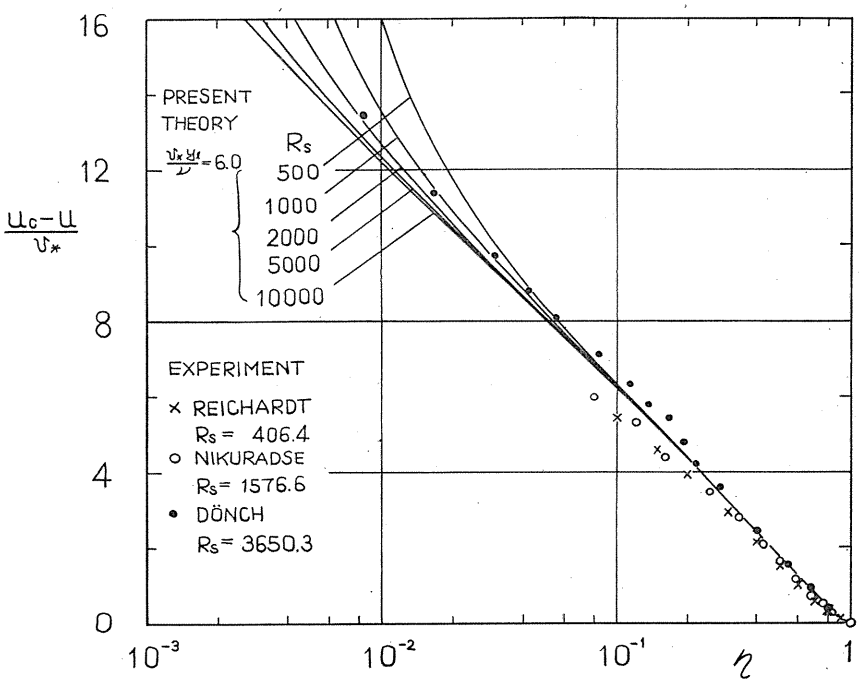

FIG. 11. Logarithmic expression of velocity defect law for $v_* y_l/\nu=6$.

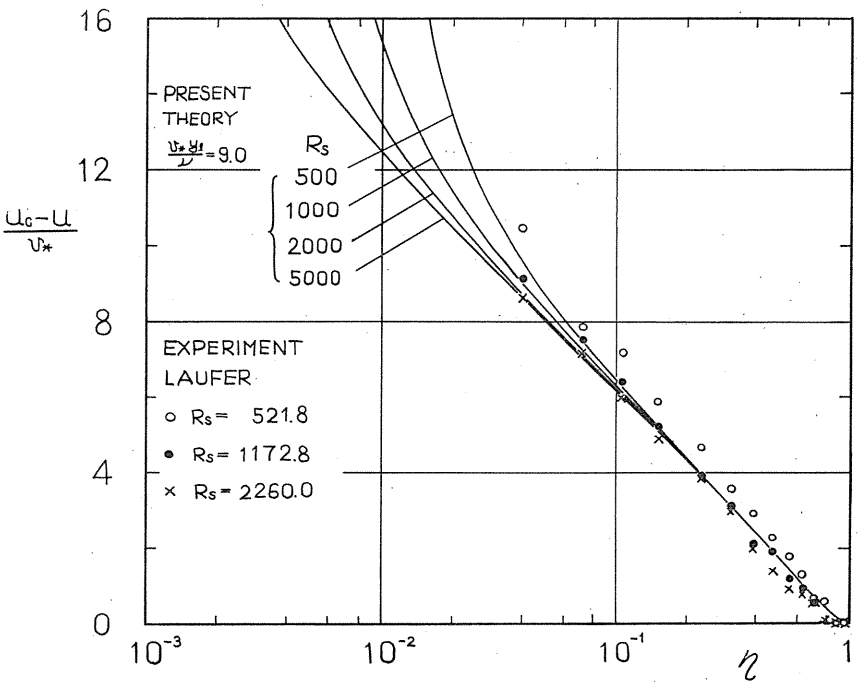

FIG. 12. Logarithmic expression of velocity defect law for $v_* y_l/\nu=9$.

5. Resistance Formula

The dimensionless coefficient of resistance in a channel is defined by:

$$\lambda \equiv -\frac{dp}{dx}\frac{2d}{\frac{1}{2}\rho u_m^2} \tag{26}$$

where u_m denotes the mean flow velocity over the channel width and d the half width of the channel. Putting $y=0$ in Eq. (5) and substituting this value of τ_0 into Eq. (26) we have

$$\lambda = \frac{4\,\tau_0}{\rho u_m^2} = 4\left(\frac{v_*}{u_m}\right)^2 \tag{27}$$

The important factor u_m/v_* is easily calculated from the known velocity distribution

$$\frac{u_m}{v_*} = \int_0^1 \frac{u}{v_*} d\eta \tag{28}$$

Thus we can calculate the resistance coefficient λ for each value of R_s. The Reynolds number R based on mean flow velocity u_m and channel width $2d$ is given by:

$$R \equiv \frac{2\,u_m d}{\nu} = 2\frac{v_* d}{\nu}\,\frac{u_m}{v_*} = 2\,R_s\left(\frac{u_m}{v_*}\right) \tag{29}$$

and is shown in Fig. 13.

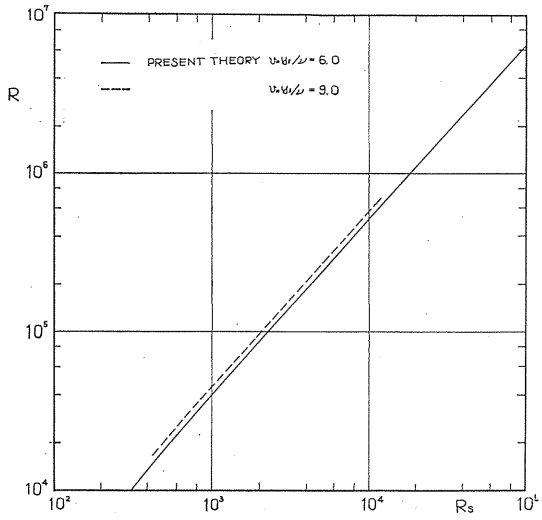

FIG. 13. Relation between R_s and R.

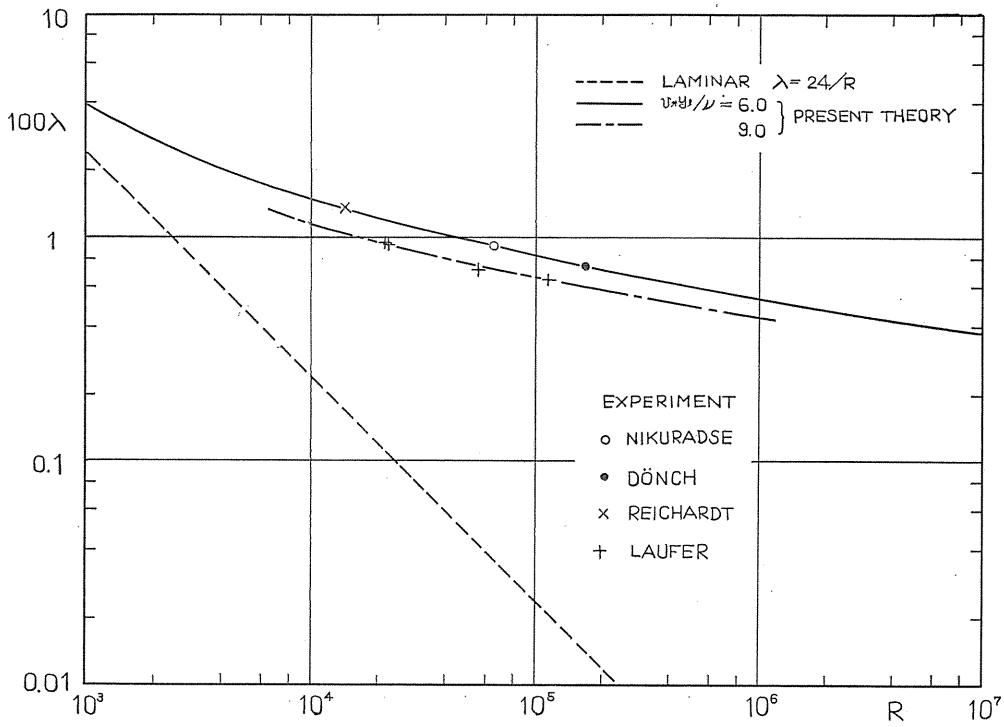

FIG. 14. The resistance formula compared with experiments.

TABLE-3. Resistance Coefficient ($v_*y_l/\nu=6$)

R_s	R	100λ
100	2.549×10^3	2.463
200	6.032×10^3	1.759
500	1.780×10^4	1.262
10^3	3.942×10^4	1.030
2×10^3	8.615×10^4	0.8623
5×10^3	$2.40\bar{5}\times10^5$	0 6917
10^4	5.148×10^5	0.6037
2×10^4	1.096×10^6	0.5333
5×10^4	2.981×10^6	0.4502
10^5	6.319×10^6	0.4008

TABLE-4. Resistance Coefficient ($v_*y_l/\nu=9$)

R_s	R	100λ
500	$2.05\bar{5}\times10^4$	0.9473
10^3	4.520×10^4	0.7833
2×10^3	9.786×10^4	0.6683
5×10^3	2.698×10^5	0.5494
10^4	5.728×10^5	0.4877

The relation between resistance coefficient λ and Reynolds number R is shown in Fig. 14 and is tabulated in Table 3 and 4. Comparing the present result with experiments[3) 4) 13) 14)] it shows fair agreement. For the convenience of practical use formulae fit to present calculation are derived from Fig. 15 for $v_*y_l/\nu=6$ and 9, respectively:

$$\left.\begin{aligned} \frac{1}{\sqrt{\lambda}} &= 2.97\log R\sqrt{\lambda}-0.83 \quad \text{at } R\geqq 3.9\times10^4 \\ \frac{1}{\sqrt{\lambda}} &= 3.06\log R\sqrt{\lambda}+0.27 \quad \text{at } R\geqq 4.5\times10^4 \end{aligned}\right\} \tag{30}$$

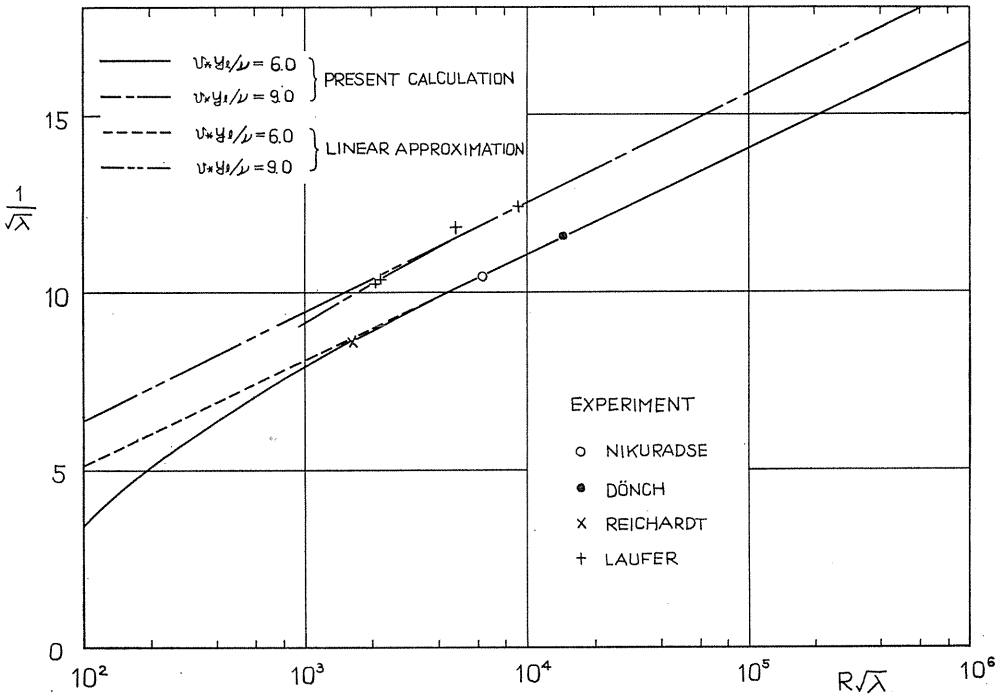

FIG. 15. The approximation of resistance formula.

6. Conclusion

A new method to calculate a turbulent flow in a two-dimensional channel is investigated. Making use of a linear expression for shearing stress and assuming polynomial expressions for mixing length, a reasonable form of velocity profile and corresponding resistance coefficient are obtained as functions of Reynolds number.

The present results seem to be explained by a few parameter, *i.e.* κ, σ and $v_* y_l/\nu$. In the present paper $v_* y_l/\nu=6$ and 9 are employed for the thickness of laminar sublayer. The experiments by Nikuradse *et al.* seem to be well represented by $v_* y_l/\nu=6$, while the experiment by Laufer is represented by $v_* y_l/\nu=9$.

References

1) L. Prandtl, Zur turbulenten Strömung in Rohren und länge Platten, Erg. Aerodyn. Vers. -Anst. zu Göttingen, IV Lief., München 1932, Oldenbourg, P. 18-29.
2) Th. von Kármán, Mechanische Ähnlichkeit und Turbulenz, Verhand. d. 3 Int. Kong. f. Tech. Mech., Stockholm 1931, Norstedt u. Söner, P. 85-93.
3) J. Nikuradse, Untersuchungen über die Strömungen des wassers in Konvergenten und Divergenten Kanälen, Forchungsarbeiten, 289, 1929.
4) J. Laufer, Investigation of turbulent flow in a two-dimensional channel, NACA TN 2124, 1950.: see also J. Laufer, Some recent Measurements in a Two-dimensional Turbulent Channel, Jour. Aero. Scie, P. 277-287, 1950.

5) J. Nikuradse, Gesetzmäßigkeit der turbulenten Strömung in glatten rohren, VDI-Forschungsheft, 356, 1932.
6) J. Laufer, The structure of turbulence in fully developed pipe flow, NACA TR 1174, 1954.
7) H. Reichardt, Vollständige Darstellung der turbulenten Geschwindigkeitsverteilung in glatten Leitungen, ZAMM **31**, P. 208-219, 1951.
8) R. G. Deissler, Analysis of turbulent heat transfer, mass transfer and friction in smooth tubes at high Prandtl and Schmidt numbers, NACA TN 3145, 1954.
9) W. Szablewski, Turbulente Stromungen in divergenten Kanälen, Ingenieur-Archiv, P. 268-281, 1954.
10) S. I. Pai, On Turbulent Flow between Parallel Plates, Jour. of Applied Mechanics P. 109-114, 1953.
11) L. Prandtl, The mechanics of viscous fluids, in W. F. Durand, Aerodynamic Theory, 142, 1953.: see also comprehensive review by L. Prandtl, Neuere Ergebnisse der Turbulenzforschung, Z. VDI 77, 105, 1933.
12) S. Uchida, K. Matsumiya, An Analysis of Turbulent Boundary Layer along a Flat Plate, Memoirs of the Faculty of Engineering, Nagoya University, **vol. 18**, No. 1, P. 34-53, 1965.
13) H. Reichardt, Messungen turbulenter Scdwankungen, Naturwissenschaften, **26**, P. 404, 1938.: see also H. Reichardt, Über das Messen turbulenter Längs- und Querschwankungen, ZAMM, 1938.
14) F. Dönch, Divergente und Konvergente turbulente Strömungen mit kleinen Öffnungswinkeln, Forschungsarbeiten, 282, 1926.